Journal of Energy Storage 31 (2020) 101615

Contents lists available at ScienceDirect

Journal of Energy Storage

journal homepage: www.elsevier.com/locate/est

Optimal scheduling of mobile utility-scale battery energy storage systems in electric power distribution networks

Hedayat Saboori, Shahram Jadid*

Center of Excellence for Power System Automation and Operation, Electrical Engineering Department, Iran University of Science and Technology, Tehran, Iran

ARTICLE INFO

Keywords:
Utility battery storage
Mobile battery storage
Optimal operation
Distribution network
Mathematical programming

ABSTRACT

Today, knowledge of battery energy storage systems (BESSs) has experienced a rapid growth resulting to the numerous grid applications. The utility-scale batteries assembled in containers can be transported in the grid. Despite numerous benefits, this feature has been overlooked. In previous studies, battery movement is modeled based on a specific transfer method, such as a truck or train. Accordingly, by changing the method of transporting the battery, the problem should be re-modeled and also it is not possible to schedule the battery movements by combining two transfer methods. In this context, this paper proposes a new battery movement scheduling in the distribution networks. To this end, optimal charging or discharging power in addition to the bus location will be determined for any time period of operation. In the proposed model, only distance between buses is important and how the battery is transferred is not important. accordingly, battery transfer may be performed using one transmission method, such as a truck or a combination of two methods (truck and train). Reactive power contribution by the battery, power losses and bus voltages of the network are also counted by maintaining linear structure of the model. This guarantees practical application of the formulation for the real-life distribution grids. Results of implementing the model on a test system indicate distinct superiority of the mobile BESS with respect to the stationary installations.

1. Introduction

Today, energy storage devices are not new to the power systems and are used for a variety of applications. Storage devices in the power systems can generally be categorized into two types of long-term with relatively low response time and short-term storage devices with fast response [1]. Each type of storage is capable of providing a specific set of applications, depending on the range of its technical parameters. The first category is suitable for energy management applications such as arbitrage, peak shipping, expansion deferral, loss reduction, island operation, renewable energy time-shift and long-term voltage control. One of the most important applications in this category is peak shaving which is thoroughly studied by the researchers [2–4].

The second category is suitable for fast power injection applications such as frequency control, stability, power conditioning, and renewable energy smoothing and grid integration. In this category, power quality is one of the most important applications which evaluated by the researchers [5]. The first category is composed of pumped hydro energy storage, compressed air energy storage as well as hydrogen storage and conversion to electricity through fuel cells. Superconducting magnetic energy storage, supercapacitor in addition to the flywheels can also be mentioned as second-class storage devices. A very high percentage of installed storage systems for energy management applications in power systems is belong to the pumped storage plant. This is due to low installation cost and also technological maturity of the pumped hydro storage. However, these installations have been mainly related to the several past decades while new installations in recent years are almost completely dedicated to the batteries. This is due to specific problems associated with the pumped hydro storage for instance environmental manipulation, high installation costs in areas without natural required structure, and the impossibility to install in the crowded urban distribution network [6]. On the contrary, the batteries are technologies which, according to design parameters, can be utilized in two categories and used for any application. The knowledge of grid-scale batteries has experienced tremendous growth over the past decade. This has led the battery to become a major player in the energy storage market in the power system, especially distribution networks [7]. The growing rate of this energy storage technology installation over the past years has shown this [8]. Their advantages include high energy density, high power density, long term energy storage, fast response, high efficiency, modular system, quiet performance, easy installation, simple energy management, quadruple active/reactive full power control, and the

* Corresponding author.
E-mail addresses: h_saboori@elec.iust.ac.ir (H. Saboori), jadid@iust.ac.ir (S. Jadid).

https://doi.org/10.1016/j.est.2020.101615
Received 18 March 2020; Received in revised form 23 May 2020; Accepted 11 June 2020

Nomenclature

Sets

A_G	set of network generators
$A_{I,\ J,\ K}$	set of network buses
$A_{T,\ U,\ V}$	set of operation time periods

Parameters

$b^{L}_{(i,j)}$	susceptance of the line between buses i and j (Siemens)
$E^{MB}_{(b)}$	rated energy of the mobile battery (kWh)
$g^{L}_{(i,j)}$	conductance of the line between buses i and j (Siemens)
$Z^{Ini}_{(i,t)}$	initial time-location status of the mobile battery
J^{Ini}	initial stored energy in the mobile battery (kWh)
$P^{BD}_{(i,\ t)}$	active power demand of bus i at time period t (kW)
$Q^{BD}_{(i,\ t)}$	reactive power demand of bus i at time period t (kVar)
$tt_{(i,\ j)}$	total battery transportation time between buses i and j (hour)
$P^{Min}_{(g)}$	minimum active power generation limit of generator g (kW)
$P^{Max}_{(g)}$	maximum active power generation limit of generator g (kW)
S^{MB}	power rating of the mobile battery (kW)
T^{BC}	charging time interval for mobile battery (hour)
T^{BD}	discharging time interval for mobile battery (hour)
$Q^{Min}_{(g)}$	minimum reactive power generation limit of generator g (kVar)
$Q^{Max}_{(g)}$	maximum reactive power generation limit of generator g (kVar)
η^{BC}	charging efficiency of the mobile battery
η^{BD}	discharging efficiency of the mobile battery
$\lambda^{NG}_{(n,g)}$	energy cost of generator g for power slice n ($/kWh)
$\lambda^{LS}_{(i,t)}$	shed load price at bus i and time period t ($/kW)

Variables

TC	total cost
$C^{NG}_{(g,\ t)}$	power generation cost of generator g at time period t ($)
$C^{LS}_{(i,\ t)}$	load shedding cost at bus i and time period t ($)
$\Delta P^{NG}_{(n,g,t)}$	slice n of power generated by generator g at time period t (kW)
$P^{BC}_{(i,\ t)}$	charged active power to the mobile battery at bus i and time period t (kW)
$P^{BD}_{(i,t)}$	discharged active power from the mobile battery at bus i and time period t (kW)
$P^{NG}_{(i,\ t)}$	total active power generated by generators located at bus i and time period t (kW)
$P^{LS}_{(i,\ t)}$	curtailed active power at bus i and time period t (kW)
$P^{MB}_{(i,\ t)}$	net active power injected by mobile battery at bus i and time period t (kW)
$P^{LF}_{(i,j,\ t)}$	active power flow of line between buses i and j at time period t (kW)
$Q^{NG}_{(i,\ t)}$	total reactive power generated by generators located at bus i and time period t (kVar)
$Q^{LS}_{(i,\ t)}$	curtailed reactive power at bus i and time period t (kVar)
$Q^{MB}_{(i,\ t)}$	net reactive power injected by mobile battery at bus i and time period t (kVar)
$Q^{BC}_{(i,\ t)}$	inductive reactive power to the mobile battery at time period t (kVar)
$Q^{BD}_{(i,\ t)}$	capacitive reactive power from the mobile battery at time period t (kVar)
$Q^{LF}_{(i,j,\ t)}$	reactive power flow of line between buses i and j at time period t (kVar)
$J^{MB}_{(t)}$	stored energy in the mobile battery at time period t (kWh)
$\nu_{(i,\ t)}$	voltage magnitude of bus i at time period t (P.U.)
$X^{BC}_{(i,t)}$	active power charging binary indicator of mobile battery at time period t
$X^{BD}_{(i,t)}$	active power discharging binary indicator of mobile battery at time period t
$Y^{BC}_{(i,t)}$	inductive reactive power charging binary indicator of mobile battery at time period t
$Y^{BD}_{(i,t)}$	capacitive reactive power discharging binary indicator of mobile battery at time period t
$Z^{MB}_{(i,t)}$	time-location binary status of mobile battery for bus i and time period t
$\delta_{(i,\ t)}$	voltage angle of bus i and time period t (Rad)

possibility to build anywhere in the distribution networks [9].

One of the unique advantages of the new grid-scale batteries is the portability. This is due to the compact structure of the batteries, where the whole system is often placed inside a container. Although this application has been used in practice recently in pilot projects [10], it has not received sufficient attention in the studies. This feature, despite its many advantages over stationary batteries, has been overlooked in the research community. This feature can improve some of the benefits of stationary batteries as well as providing new applications. Mobile battery benefits for the utility, costumers, and society can be classified as follows.

Utility

- Promote renewable energy by offering location shift in addition to the time shift of the production time.
- Enhanced efficient use of network capacity by removing charging and discharging power of the conventional stationary batteries.
- Enhanced peak shaving and less expensive and pollutants peak power production.
- Defer expansion requirements as a consequence of the peak shaving.
- Less power losses and higher efficiency of the network.
- Higher power quality through less voltage drop.

Costumers

- Lower energy prices through load leveling
- Reduce congestion and enhanced grid access for the consumers.
- Enhanced reliability by offering back-up power in case of emergencies.
- More resilient service irrespective of the climate situation.

Society

- Enable faster construction by providing power needed for the construction at the remote areas without access to the grid.
- Promote economic growth by preventing loss of work days during periods of power outages.
- Support centers of refuge in regional crises by forming first responders.
- Promote electric vehicle adoption by supplying remote and/or mobile charging stations.
- Helping to counter climate change by promoting clean energy, higher EV adoption, more efficient grids, less power losses, and less pollutant peak power generators.

The authors in [11–13] have been conducted similar studies on mobile storage systems. The main model is proposed in [11] wherein a unit commitment framework is proposed for mobile battery operation in transmission networks. The mobile battery is transported via railways and tries to enhance economics and technical features of the

network. Afterwards, the authors in [12] have been proposed a Lagrangian decomposition technique to solve the model. The IEEE 118 bus network in conjunction with an 8-station and 10-line railway system is used as case study. The same authors in [13] have expanded their model to consider uncertainties. Therefore, a scenario-based stochastic programming is proposed to handle two type of uncertainties. The first one is uncertainties related to the inaccuracies in forecasting load and wind energy. The second one is forced outages because of disturbances including generators, lines, and railway stations and lines. Finally, a Monte Arlo Simulation (MCS) is used for scenario tree modeling.

An optimal sizing model is introduced in [14] for transportable battery storages. The model aims at two objectives, namely reliability enhancement and energy saving. Penetration of renewable resources is considered and the model is implemented based on a distribution network. In [15], an operation model is proposed for both stationary and mobile battery systems in distribution networks. Then, based on the proposed operation model, a planning model is proposed to optimally size the batteries. In this regard, a cost-benefit analysis is performed based on batteries benefits and costs.

The mobile batteries in various research studies are used to enhance network resiliency. Power system resilience denotes the capability to withstand, adapt, and quickly recover from interruptions [16]. The interruptions in this category are mainly low-probability and high-impact events for instance natural disasters, large-scale cyber-attacks, or intentional human sabotages [17]. For example, the author in [18] have been employed mobile battery storage system to enhance network resilience. Thus, a joint investment planning and operation scheduling procedure is proposed for mobile batteries. In this regard, a two-stage optimization model which aims at maximizing network resilience but with minimum investment cost is introduced. The mobile batteries enhance network resilience by partitioning network via forming dynamic microgrids. A similar work is proposed in [19] for augmenting grid resilience by using mobile batteries. To this end, a coordinated post-disaster recovery paradigm, microgrid generation rescheduling, and network reconfiguration is proposed. The proposed model aims at minimizing projected costs including interruption cost, generation cost, and battery costs. A temporal-spatial model is proposed which models transportation network in conjunction with power grid.

In [20] a two-stage scheduling procedure is introduced for resilient operation of mobile power sources in distribution networks including batteries. In the first stage, mobile sources are pre-positioned to support rapid restoration of the disruptions which in turn assist to survive critical loads. In the second stage, i.e., after the event, the mobile power sources will be dispatched in a coordinated manner to enhance restored load.

Although one of the most important applications of mobile batteries is to improve reliability and resilience in emergencies, it should be noted that operating them under normal network conditions has also numerous benefits that have been disregarded. In addition, the proposed models for battery time-location management are all based on modeling a specific transportation network and linking it to the electricity grid. This issue has the following disadvantages. First, due to considering only one specific transport network, the number of effective network connection points is reduced. It is also not possible to examine and use a combination of mediums of transport. Furthermore, this method has the limitations of not being able to compare traffic patterns with each other.

Therefore, new mathematical models are needed to be presented and analyzed. Accordingly, this paper presents a new time- location model for optimal utilization of mobile batteries in the power distribution network. The proposed model for battery transport management is integrated in the optimal power flow (OPF) model to be used concurrently as one of the network control variables along with other ones. The model proposed for transporting batteries is independent from the transportation network. In this case, it is possible to evaluate different types of transport networks, compare them with each other, or combine them. Various features of real-life grid-scale batteries are modeled, including the ability to inject and draw reactive power and full quadruple active/reactive operation. The proposed model is a Mixed Integer Linear Programming (MILP) model which ensures convergence in very large scale real-life distribution networks. Also, the grid voltage, reactive voltages and losses calculated and considered while maintaining linear structure of the formulation. In summary, paper innovations can be listed as follows:

- Novel time-location modeling of mobile batteries based on integer modeling
- Optimal mobile battery storage scheduling in distribution networks
- New time-location model for the battery independent of the traffic medium

  Considering battery reactive power exchange besides active power

- Linear model capable of handling very large-scale real-life systems

After this introduction and in Chapter 2, the proposed model has been fully elucidated. This chapter first describes the physical concept of time-location battery management and then proposes and analyzes the mathematical relationships. Then, in Chapter 3, a case study is performed using the proposed formulation on a test network. This chapter first presents the problem inputs including constants and parameters and then presents the results of simulations. Then, in Chapter 4 a discussion is made on the results of the simulation. Finally, in Chapter 5, a summary of the study findings is presented.

2. The proposed model

This chapter is dedicated to introducing a conceptual and mathematical model of the time-location scheduling of a mobile battery and its optimal operation in the distribution network. The model inputs are network data inducing loads, substation, and lines in addition to the parameters related to the mobile battery. The outputs of the model are hourly active and reactive power output of the substation, battery hourly location and charging/discharging powers, bus voltages, and variables related to the lines including active and reactive power flows and losses. The decision variables of the problem are battery location, battery charging and discharging power and hourly bus shed load. Objective function of the problem reflects daily operation cost while constraints are related to the physical limitation of the network lines, mobile battery, and power balance.

Initially, the basic rules of time-location modeling of the mobile battery will be presented and then the related mathematical relationships will be extracted. Although the changes in battery power are not without dynamics [21], a steady-state operation model is used here to optimize the battery operation. This model is based on input-output equations and is quite common in optimization studies. Then the proposed model for the mobile battery will be integrated in the optimal power flow problem of the distribution network. At the end of the section, the total proposed formulation is summarized and inputs and outputs of the model are introduced.

2.1. Mobile battery storage transportation modeling

Optimal operation of the mobile batteries in the distribution network demands proper time-location modeling. Fig. 1 shows the pattern of the time-location movement of a battery. Each of the circles marked with two numbers inside it displays a time-location status for the battery. Ideally, all possible transfers are considered on the figure. In practice, some transfers may be impossible for technical reasons. This may be due to the lack of enough space to place the battery in the desired location or the lack of battery connection equipment.

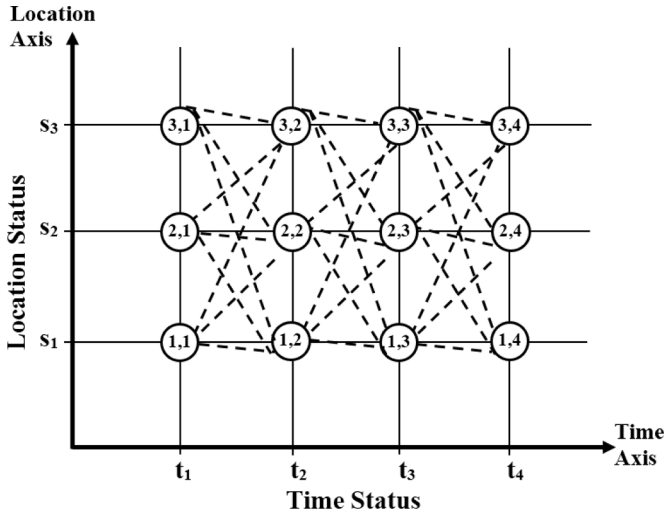

Fig. 1. Time-location status of the mobile battery storage system.

Each time-location status can be specified by a binary variable with two dimensions of time and location. If the value of the binary variable is equal to 1, it means that the battery was present at the designated location at the labelled time. If the variable value is zero, it means that the battery was moving between the two locations. Thus, time-location status of the battery takes values 0 and 1 as follows.

$$Z_{(i,t)}^{MB} \in \{0, 1\} \quad \forall \ t \in A_T \ , \ i \in A_I \tag{1}$$

It should be noted that each mobile battery cannot connect to more than one bus at any time period. This is mathematical modeled by using a special-ordered-set (SOS) in (12).

$$\sum_{i} Z_{(i,t)}^{MB} \le 1 \quad \forall \ t \in A_T \tag{2}$$

The preliminary condition for transportation between two network buses is to meet the minimum time required for transmission between those two locations. The required time for transportation is itself composed of the following time components.

a Disconnecting the battery from the present bus
b Loading the battery in the present bus location
c Movement time between two present and new bus location
d Unloading the battery in the new bus location
e Connecting the battery to the new bus

The abovementioned cost components are almost similar for the various movements except for the item 3, namely movement time. In other word, the time spent for battery disconnection, loading, unloading, and connecting is constant for all movements. Therefore, transportation time between two arbitrary buses can be wrote as (3). In this equations, $tt_{(i,\ j)}$, t^{Di}, t^{Lo}, $tt_{(i,j)}^{Tr}$, t^{Un}, and t^{Co}denote total movement time between buses i and j, disconnection time, loading time, transportation time between buses, unloading time, and connecting time of the battery, respectively.

$$tt_{(i,j)} = t^{Di} + t^{Lo} + t_{(i,j)}^{Tr} + t^{Un} + t^{Co} \quad \forall \ i, j \in A_I \tag{3}$$

As a result, total time required for each movement for all possible transportation can be presented by a matrix. This matrix, titled Movement Time Matrix (MTM), is shown in (3).

$$MTM = \begin{bmatrix} tt_{1,1} & tt_{1,2} & tt_{1,3} & \ldots & tt_{1,J} \\ tt_{2,1} & \ldots & \ldots & \ldots & \ldots \\ tt_{3,1} & \ldots & \ldots & \ldots & \ldots \\ \ldots & \ldots & \ldots & \ldots & \ldots \\ tt_{I,1} & \ldots & \ldots & \ldots & tt_{I,J} \end{bmatrix} \quad \forall \ i, j \in A_I \tag{4}$$

Each element in the MTM matrix, $tt_{(i,j),}$ represents total time required for the designated movement which is introduced previously. In the matrix, rows and columns are the origin and destination locations, respectively. Two important points about this matrix are:

a Elements on the original diameter of the matrix mean moving to the current location and thus having a value of zero.
b Symmetric elements are not necessarily equal, meaning that the time required to transfer between the origin and destination is not necessarily the same in both directions.
c An impossible movement can be represented by an infinity value for the corresponding movement.

It should be noted that, each time period in the time-location battery management problem is a stamp of the network buses (locations). Any battery movement means transport from a bus location in the present stamp to any other bus locations (not equal to the present) in one of the next time periods (stamps). It should be noted that the battery cannot move between two successive time periods because of transport time limitation. In other word, transportation between two buses need at least a single time period. For any transport from bus i to j with transport time $tt_{(i,j),}$ which take places between two non-successive time periods t and u, two conditions should be met as follows.

a Associated time-location binary variables for origin and destination time periods should be equal to 1 at least for one of the network buses. Mathematically speaking:

$$\sum_{i} Z_{(i,t)}^{MB} = 1 \quad \forall \ t \in A_T \tag{5}$$

$$\sum_{j} Z_{(i,u)}^{MB} = 1 \quad \forall \ u \in A_T \tag{6}$$

b Considering that total transport time between two buses is at least a large as a single time period, destination time should be greater than the origin time in addition to at least two time periods. In other word:

$$u \ge t + 2 \ , \ \forall \ tt_{(i,j)} \ge 1 \tag{7}$$

c There should be at least as much difference as the entire time of transfer (namely $tt_{(i,j),}$) between the origin and destination time periods of the movement. Considering that total transport time between two buses is at least a large as a single time period, this condition also necessitates the previous condition. This can be shown mathematically as:

$$u \ge t + tt_{(i,j)} + 1 \ , \ \forall \ tt_{(i,j)} \ge 1 \tag{8}$$

d In the whole time of transport, which is at least as equal as the $tt_{(i,j),}$ the battery is disconnected from the network and therefore all associated binary variables should be equal to zero. This can be mathematically expressed by:

$$\sum_{v,i} Z_{(i,v)}^{MB} = 0 \quad \forall \ t + 1 \le v \le t + tt_{(i,j)} \tag{9}$$

e Origin and destination buses should not be the same as established in the following inequality.

$$i \ne j \quad \forall \ \{t, u\} \in A_T \tag{10}$$

The abovementioned conditions should be met simultaneously for

any arbitrary transport of the battery. All of above conditions can be merged into some general relations. This is performed in (11) and (12).

$$Z^{MB}_{(i,t)} + Z^{MB}_{(j,u)} \le 1 \quad \forall\ t \in A_T\ ,\ \{i,j\} \in A_I\ ,\ i \ne j\ ,$$
$$u = \{t+1,\ ...,t + ToT_{(i,j)}\} \tag{11}$$

$$\sum_{u=t+1}^{t+ToT_{(i,j)}+1} [Z^{MB}_{(j,u)}] \ge Z^{MB}_{(i,t)} \quad \forall\ t \in A_T\ ,\ \{i,j\} \in A_I \tag{12}$$

In (11) and (12) all of necessary transportation conditions introduced in (5) to (10) are modeled and considered. By using these two new relations, any battery transport in the network will be confined by the transportation time. Another point is that the battery will start scheduling period with a predefined location at the beginning of the time periods. Also, at the end of the scheduling, it should be relocated to the initial location to start another day. These two situation are mathematically expressed in (13) and (14).

$$Z^{MB}_{(i,tt)} = Z^{Ini}_{(i,t)} \quad \forall\ i \in A_I\ ,\ \ t \in A_T,\ \ tt = t_0 \tag{13}$$

$$Z^{MB}_{(i,tt)} = Z^{Ini}_{(i,t)} \quad \forall\ i \in A_I\ ,\ \ t \in A_T,\ \ tt = t_T \tag{14}$$

The battery can exchange power if it is not in transit and connected to one of the network buses. Also, if the battery is connected to one of the network buses, it can only charge or discharge at a time period. In other word, the battery charging and discharging cannot occur simultaneously over a period of time. These conditions are defined in (15) by using two binary variables for charging and discharging of active power. In addition, (16) and (17) necessitate that the battery can be charged or discharged if the relevant binary variable is switched on. This requires that the battery is already connected to the corresponding network bus. Inequalities (16) and (17) also point out that the battery cannot exceed the rated power in the charge and discharge state.

$$X^{BC}_{(i,t)} + X^{BD}_{(i,t)} \le Z^{MB}_{(i,t)} \quad \forall\ i \in A_I\ ,\ \forall\ t \in A_T \tag{15}$$

$$P^{BC}_{(i,t)} \le X^{BC}_{(i,t)}\ S^{MB} \quad \forall\ i \in A_I\ ,\ \forall\ t \in A_T \tag{16}$$

$$P^{BD}_{(i,t)} \le X^{BD}_{(i,t)}\ S^{MB} \quad \forall\ i \in A_I\ ,\ \forall\ t \in A_T \tag{17}$$

The conditions described for active power also apply to reactive power. In other word, only if the battery is connected to the grid and the relevant binary variable is turned on will the battery be able to perform a reactive power injection or withdrawal action. These situations are mathematically modeled in (18) to (20).

$$Y^{BC}_{(i,t)} + Y^{BD}_{(i,t)} \le Z^{MB}_{(i,t)} \quad \forall\ i \in A_I\ ,\ \forall\ t \in A_T \tag{18}$$

$$Q^{BC}_{(i,t)} \le Y^{BC}_{(i,t)}\ S^{MB} \quad \forall\ i \in A_I\ ,\ \forall\ t \in A_T \tag{19}$$

$$Q^{BD}_{(i,t)} \le Y^{BD}_{(i,t)}\ S^{MB} \quad \forall\ i \in A_I\ ,\ \forall\ t \in A_T \tag{20}$$

The net active or reactive power injected by the battery is equal to the difference between its charging and discharging powers. Eqs. (21) and (22) illustrate this for each time interval and each mobile battery in the network.

$$P^{MB}_{(i,t)} = P^{BD}_{(i,t)} - P^{BC}_{(i,t)} \quad \forall\ i \in A_I\ ,\ \forall\ t \in A_T \tag{21}$$

$$Q^{MB}_{(i,t)} = Q^{BD}_{(i,t)} - Q^{BC}_{(i,t)} \quad \forall\ i \in A_I\ ,\ \forall\ t \in A_T \tag{22}$$

It should be noted that the vector of the active and reactive power in both the charge and discharge states should not exceed the rated power of the battery. This can be shown by using defined net active and reactive power of the battery, as in (23). This inequality is the apparent power limitation of the battery which can be rewritten as (24).

$$\sqrt{(P^{MB}_{(i,t)})^2 + (Q^{MB}_{(i,t)})^2} \le S^{MB} \quad \forall\ i \in A_I\ ,\ \forall\ t \in A_T \tag{23}$$

$$(P^{MB}_{(i,t)})^2 + (Q^{MB}_{(i,t)})^2 \le (S^{MB})^2 \quad \forall\ i \in A_I\ ,\ \forall\ t \in A_T \tag{24}$$

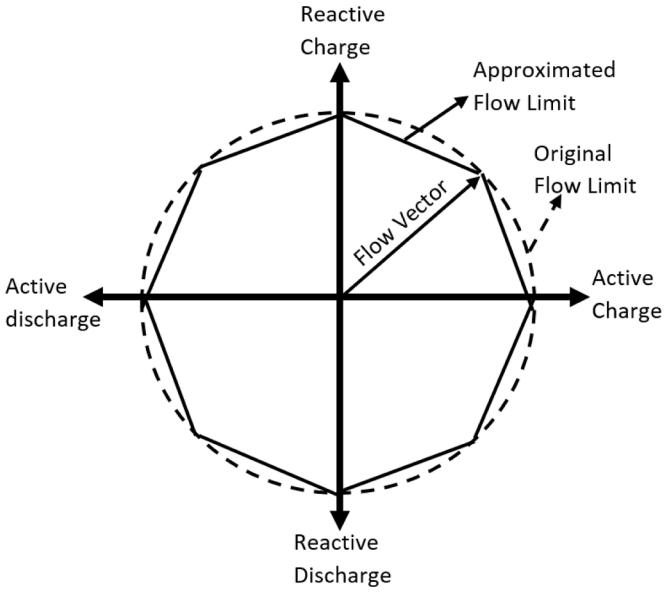

Fig. 2. Battery apparent power flow limit and approximation.

The relation introduced in (24), which is non-linear, is shown in Fig. 2 where its interpretation is locus of the point inside a circle. Each point within the circle is a combination of the active and reactive power of the battery and the radius is equal to the rated power of the battery. To avoid non-linearity, the binding circle can be approximated by a set of straight lines constituting a polygon. As illustrated in the figure, the linear version of the circle is a convex regular polygon with m sides. Enhancing sides of the polygon will increase approximation accuracy at the expense of the computation time. By defining equation of each side of polygon and then applying some manipulation and simplification, the original non-linear relation in (24) can be rewritten as (25) which is linear. More details can be found in [22, 23]

$$\frac{\mathrm{Cos}\frac{(2m-1)\pi}{M} P^{MB}_{(i,t)} + \mathrm{Sin}\frac{(2m-1)\pi}{M} Q^{MB}_{(i,t)}}{\mathrm{Cos}(\pi/M)} \le S^{MB}$$
$$\forall\ \ m \in A_M\ ,\ \ \forall\ i \in A_I\ ,\ \forall\ t \in A_T \tag{25}$$

Final stage in the battery modeling is defining battery energy conditions. The first point is that, similar to the battery location, the battery starts the time periods with a predefined stored energy and ends with the same value. These two conditions for initial and final stored energy are dented by (26) and (27), respectively.

$$J^{MB}_{(t)} = J^{Ini} \quad \forall\ t = t_0 \tag{26}$$

$$J^{MB}_{(t)} = J^{Ini} \quad \forall\ t = t_T \tag{27}$$

Stored energy in the battery at any time period is equal to the previously stored energy in addition to the net energy absorbed at the present time period. The net absorbed energy is itself difference between drawn energy and injected energy, as declared in (28). Additionally, stored energy at any time period should be a positive value and cannot exceed rated energy of the battery, as in (29). Finally, energy injected by the battery to the grid should be lower than the total stored energy, as shown in (30) [24, 25]. It should be noted that the reactive power production by the battery is not considered here because of its negligible value.

$$J^{MB}_{(t)} = J^{MB}_{(t-1)} + \sum_i P^{BC}_{(i,t)}\ T^{BC}\eta^{BC} - \sum_i P^{BD}_{(i,t)}\ T^{BD}/\eta^{BD} \quad \forall\ t \in A_T \tag{28}$$

$$0 \le J^{MB}_{(t)} \le E^{MB} \quad \forall\ \ t \in A_T \tag{29}$$

$$P^{BD}_{(i,t)}\ T^{BD} \le J^{MB}_{(t)}\eta^{BD} \quad \forall\ \ t \in A_T \tag{30}$$

2.2. Integrating mobile battery model in the optimal power flow problem

The aim of optimal power flow (OPF) problem is to find the minimum cost operation schedule of the network for a specific time window which is itself composed of several time intervals [26]. Various studies have been work on the energ7y storage integration in the OPF problem [27,28]. In the present work, the relation between the OPF problem and the energy storage model is built based on the nodal power balance equations. This will be explained in the following. Objective function of the problem which is daily operation cost is defined in (31). As in the equation, daily operation cost is composed of the cost terms elaborated over all time periods, namely total energy cost of the network generators and total cost of the load shedding.

$$TC = \sum_{g,t} C^{NG}_{(g,t)} + \sum_{i,t} C^{LS}_{(i,t)} \tag{31}$$

Based on popular approach, it is assumed that power generation cost of each network generator follows a stair-wise paradigm. Each stair of generated power has its own generation cost wherein increases with the amount of the generated power [29]. Total cost of power generation is equal to the summation over cost of each step of generated power, as denoted by (32). Accordingly, total generated power will be equal to the summation over all powers generated in the steps which is modeled in (33). Active and reactive power generated by each generator are limited by the corresponding upper and lower limits as shown by (34) and (35).

$$C^{NG}_{(g,t)} = \sum_{n} \lambda^{NG}_{(n,g)} \Delta P^{NG}_{(n,g,t)} \quad \forall\ g \in A_G\ ,\ \forall\ t \in A_T \tag{32}$$

$$P^{NG}_{(g,t)} = \sum_{n} \Delta P^{NG}_{(n,g,t)} \quad \forall\ g \in A_G\ ,\ \forall\ t \in A_T \tag{33}$$

$$P^{Min}_{(g)} \le P^{NG}_{(g,t)} \le P^{Max}_{(g)} \quad \forall\ g \in A_G\ ,\ \forall\ t \in A_T \tag{34}$$

$$Q^{Min}_{(g)} \le Q^{NG}_{(g,t)} \le Q^{Max}_{(g)} \quad \forall\ g \in A_G\ ,\ \forall\ t \in A_T \tag{35}$$

For whatever reason, the demand load on a bus may not be met and will be forcibly disconnected by the network operator. In this case, there will be a payment to the curtailed costumer by the network operator. This cost, known as load shedding cost, is a function of the amount of curtailed load as well as the value of the electric energy shed which is modeled in (36). As shown in (37) and (38), the shed load cannot be greater than the bus active and reactive load. In other word, it cannot be negated and play the role of a power source. Also, the ratio of the reactive power shed in the bus must be precisely as equal as the active power, which is mathematically modeled in (39).

$$C^{LS}_{(i,t)} = \lambda^{LS}_{(i)} P^{LS}_{(i,t)} \quad \forall\ i \in A_I\ ,\ \forall\ t \in A_T \tag{36}$$

$$0 \le P^{LS}_{(i,t)} \le P^{BD}_{(i,t)} \quad \forall\ i \in A_I\ ,\ \forall\ t \in A_T \tag{37}$$

$$0 \le Q^{LS}_{(i,t)} \le Q^{BD}_{(i,t)} \quad \forall\ i \in A_I\ ,\ \forall\ t \in A_T \tag{38}$$

$$Q^{LS}_{(i,t)} = (P^{LS}_{(i,t)}/P^{BD}_{(i,t)}) Q^{BD}_{(i,t)} \quad \forall\ i \in A_T\ ,\ \forall\ t \in A_T \tag{39}$$

Another physical characteristic of the network which should be modeled is power balance. It means that balance between generated and consumed power in any bus of the network should be kept at any time period. This is mathematically expressed by (40) and (41) for active and reactive powers, respectively. As in the equations, generations in the bus include power generated by the installed generators, curtailed load, and net power injected by the mobile battery. On the contrary, bus load and net power flow leaving the bus constitute consumption of the bus.

$$\sum_{g \in A_{GI}} P^{NG}_{(i,t)} + P^{LS}_{(i,t)} + P^{MB}_{(i,t)} = P^{BD}_{(i,t)} + \sum_{j} P^{LF}_{(i,j,t)} \quad \forall\ i \in A_I\ ,\ \forall\ t \in A_T \tag{40}$$

$$\sum_{g \in A_{GI}} Q^{NG}_{(i,t)} + Q^{LS}_{(i,t)} + Q^{MB}_{(i,t)} = Q^{BD}_{(i,t)} + \sum_{j} Q^{LF}_{(i,j,t)} \quad \forall\ i \in A_I\ ,\ \forall\ t \in A_T \tag{41}$$

Finally, active and reactive power flow in each line of the network can be easily calculated by (42) and (43). These are approximated linear versions of the original non-linear newton model of the power flow equations. More details on the linearization technique and accuracy analysis can be found in [30,31].

$$P^{LF}_{(i,j,t)} = g^{L}_{(i,j)} [\nu_{(i,t)} - \nu_{(j,t)}] - b^{L}_{(i,j)} [\delta_{(i,t)} - \delta_{(j,t)}] + g^{L}_{(i,j)} \left[\left(\frac{(\delta_{(i,t)} - \delta_{(j,t)})^2}{2} \right) + \left(\frac{(\nu_{(i,t)} - \nu_{(j,t)})^2}{8} \right) \right] \quad \forall\ i \in A_I\ ,\ \forall\ t \in A_T \tag{42}$$

$$Q^{LF}_{(i,j,t)} = -b^{L}_{(i,j)} [\nu_{(i,t)} - \nu_{(j,t)}] - g^{L}_{(i,j)} [\delta_{(i,t)} - \delta_{(j,t)}] + -b^{L}_{(i,j)} \left[\left(\frac{(\delta_{(i,t)} - \delta_{(j,t)})^2}{2} \right) + \left(\frac{(\nu_{(i,t)} - \nu_{(j,t)})^2}{8} \right) \right] \quad \forall\ i \in A_I\ ,\ \forall\ t \in A_T \tag{43}$$

2.3. Summarization and model characterization

The model formulated in the previous sub-sections tries to minimize daily operation cost of the distribution network by optimal scheduling of the mobile battery storage. The model can be simplified generally as follows.

$$\textit{Minimize } TC \qquad \textit{Subjected to: } \begin{cases} (1) - (2) \\ (11) - (22) \\ (25) - (43) \end{cases} \tag{44}$$

The above optimization problem is mixed integer linear programming (MILP) model which can easily solve using available commercial packages. Inputs of the model are network parameters in addition to the mobile battery characteristics which are totally describes in details in the subsequent section. Main output of the model is time-location scheduling of the mobile battery which yields in turn other network variables including power generations, flows, losses, and bus voltages.

3. Case study

In this section, the introduced in the previous section is tested on a sample case. Initially, the constants and input parameters of the problem are introduced and their values are defined. Then the simulation results are presented and analyzed.

3.1. Description of the case study

The IEEE 33 bus distribution test system is used for case study. Layout of the system is depicted in Fig. 3 and Table 1 shows line and load data [32]. Total system load is equal to 3715 kW and 2300 kVar for active and reactive power. Total bus demand is subjected to the hourly load factor which is depicted in Fig. 4. The system is supplied via the up-stream substation with the stair-wise energy cost shown in Fig. 5. [33]. Operation time window is a day consist of 24 one-hour time periods. A mobile battery with zero initial stored energy and located at bus 1 of the system at the beginning of the time periods is supposed. Power rating of the mobile battery is equal to 750 kW and with 2000 kWh energy capacity. Furthermore, charging and discharging efficiency of the battery are equal to 0.95. It is supposed that required footprint and technical connection equipment for the mobile battery are provided in buses 1, 3, 6, 12, 20, 24, and 30 of the network which covers almost all areas of the system. For the sake of simplicity and ease of analyzing results total transportation time for all possible movements is assumed to be one hour. The CPLEX [34] solver within

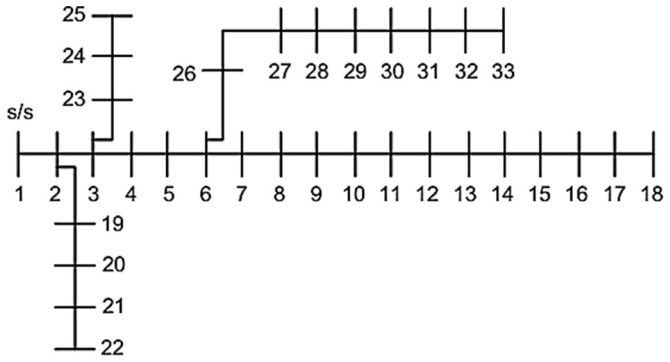

Fig. 3. IEEE 33-bus distribution test case.

Table 1
Line and load data for IEEE 33-bus system.

Line Location		Line Parameters		Bus Loads at Receiving Bus	
Sending Bus	Receiving Bus	R (Ω)	X (Ω)	P (kW)	Q (kVar)
1	2	0.0922	0.047	100	60
2	3	0.493	0.2511	90	40
3	4	0.366	0.1864	120	80
4	5	0.3811	0.1941	60	30
5	6	0.819	0.707	60	20
6	7	0.1872	0.6188	200	100
7	8	0.7114	0.2351	200	100
8	9	1.03	0.74	60	20
9	10	1.044	0.74	60	20
10	11	0.1966	0.065	45	30
11	12	0.3744	0.1238	60	35
12	13	1.468	1.155	60	35
13	14	0.5416	0.7129	120	80
14	15	0.591	0.526	60	10
15	16	0.7463	0.545	60	20
16	17	1.289	1.721	60	20
17	18	0.732	0.574	90	40
2	19	0.164	0.1565	90	40
19	20	1.5042	1.3554	90	40
20	21	0.4095	0.4784	90	40
21	22	0.7089	0.9373	90	40
3	3	0.4512	0.3083	90	50
23	24	0.898	0.7091	420	200
24	25	0.896	0.7011	420	200
6	26	0.203	0.1034	60	25
26	27	0.2842	0.1447	60	25
27	28	1.059	0.9337	60	20
28	29	0.8042	0.7006	120	70
29	30	0.5075	0.2585	200	600
30	31	0.9744	0.963	150	70
31	32	0.3105	0.3619	210	100
32	33	0.341	0.5302	60	40

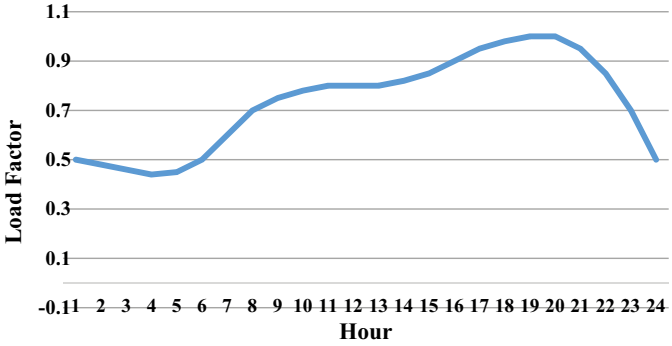

Fig. 4. Hourly load factor.

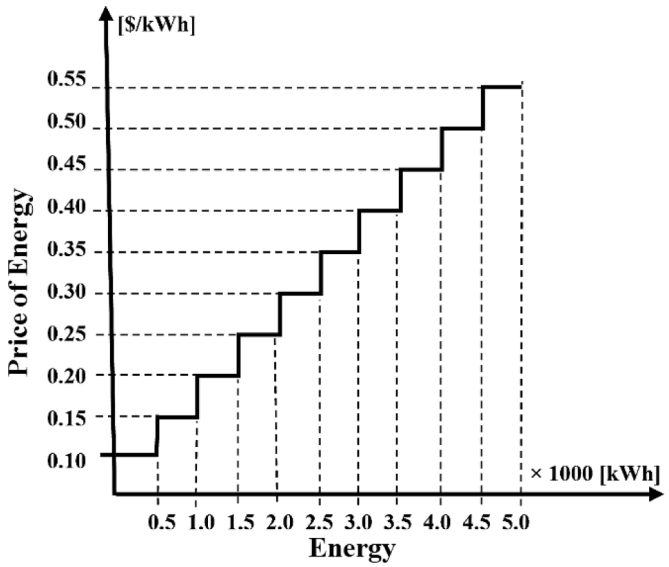

Fig. 5. Step-wise generation cost function [29].

the GAMS [35] environment is used to implement and solve the model formulation. Accordingly, Movement Time Matrix (MTM) is presented in Table 2.

3.1. Simulation results

The model is simulated for three cases. The first one is a distribution network without battery storage, titled as NBESS (no battery energy storage system). The second one is case wherein a stationary battery energy storage is installed at one of the system buses, title as SBESS (stationary battery energy storage system). The third one which is the main case is titled as BESS (mobile battery storage operation). Results of the three above-mentioned cases are compared to evaluate functionality of the proposed model.

Table 3 represents total simulation results for all cases. The table reports total daily operation cost as well as location of the mobile batteries. Additionally, difference between total cost of each case with case NBESS are shown in terms of dollars and percent. Based on the results, total daily operation cost for the conventional distribution grid without battery storage is equal to 16,841 dollars. As in the table, mobile operation of the battery will reduce daily operation cost by 683 dollars. This means that a 4.06 percent net reduction with respect to the case without battery storage in the network, namely NBESS. In this case, the battery interacts with the grid at the 1 and 30 buses. If the battery performs charging and discharging actions in the same location for any time period, i.e., a stationary installation, results will be different based on the battery bus location. Fig. 6 represents total cost reduction percent for various bus locations of the stationary battery. As in the figure, cost reduction is at most 3.6 percent which is lower than the mobile battery. The figure also implies that stationary battery installation at buses 6–12 and 26–33 offer higher cost reduction but all lower than the mobile battery. As last rows of Table 3 presents, stationary battery installation can yield at most 3.60 cost reduction at bus 30 of the network. Additionally, installation at bus 1 has the lowest impact on the total daily cost. This is due to the fact that in this case the down-stream network catches the least impact from the battery installation. Also the table reports average and median values of the cost reduction for all b uses of the network, namely 2.91 and 3.30 percent. As the results verify, mobile operation of the battery offers a distinct and considerable advantage over the stationary installation in all its locations. It should be noted that the achieved benefits by employing mobile battery storage will be increased by increasing battery efficiency. As it was stated previously, charging and discharging efficiency

Table 2
Movement Time Matrix (MTM) for the studied case.

	1	2	3	4	5	6	7	8	9	10	11	12	13	14	15	16	17	18	19	20	21	22	23	24	25	26	27	28	29	30	31	32	33
1	0	∞	1	∞	∞	1	∞	∞	∞	∞	∞	1	∞	∞	∞	∞	∞	∞	∞	1	∞	∞	∞	1	∞	∞	∞	∞	∞	1	∞	∞	∞
2	∞	0	∞	∞	∞	∞	∞	∞	∞	∞	∞	∞	∞	∞	∞	∞	∞	∞	∞	∞	∞	∞	∞	∞	∞	∞	∞	∞	∞	∞	∞	∞	∞
3	1	∞	0	∞	∞	1	∞	∞	∞	∞	∞	1	∞	∞	∞	∞	∞	∞	∞	1	∞	∞	∞	1	∞	∞	∞	∞	∞	1	∞	∞	∞
4	∞	∞	∞	0	∞	∞	∞	∞	∞	∞	∞	∞	∞	∞	∞	∞	∞	∞	∞	∞	∞	∞	∞	∞	∞	∞	∞	∞	∞	∞	∞	∞	∞
5	∞	∞	∞	∞	0	∞	∞	∞	∞	∞	∞	∞	∞	∞	∞	∞	∞	∞	∞	∞	∞	∞	∞	∞	∞	∞	∞	∞	∞	∞	∞	∞	∞
6	1	∞	1	∞	∞	0	∞	∞	∞	∞	∞	1	∞	∞	∞	∞	∞	∞	∞	1	∞	∞	∞	1	∞	∞	∞	∞	∞	1	∞	∞	∞
7	∞	∞	∞	∞	∞	∞	0	∞	∞	∞	∞	∞	∞	∞	∞	∞	∞	∞	∞	∞	∞	∞	∞	∞	∞	∞	∞	∞	∞	∞	∞	∞	∞
8	∞	∞	∞	∞	∞	∞	∞	0	∞	∞	∞	∞	∞	∞	∞	∞	∞	∞	∞	∞	∞	∞	∞	∞	∞	∞	∞	∞	∞	∞	∞	∞	∞
9	∞	∞	∞	∞	∞	∞	∞	∞	0	∞	∞	∞	∞	∞	∞	∞	∞	∞	∞	∞	∞	∞	∞	∞	∞	∞	∞	∞	∞	∞	∞	∞	∞
10	∞	∞	∞	∞	∞	∞	∞	∞	∞	0	∞	∞	∞	∞	∞	∞	∞	∞	∞	∞	∞	∞	∞	∞	∞	∞	∞	∞	∞	∞	∞	∞	∞
11	∞	∞	∞	∞	∞	∞	∞	∞	∞	∞	0	∞	∞	∞	∞	∞	∞	∞	∞	∞	∞	∞	∞	∞	∞	∞	∞	∞	∞	∞	∞	∞	∞
12	1	∞	1	∞	∞	∞	∞	∞	∞	∞	∞	0	∞	∞	∞	∞	∞	∞	∞	1	∞	∞	∞	1	∞	∞	∞	∞	∞	1	∞	∞	∞
13	∞	∞	∞	∞	∞	∞	∞	∞	∞	∞	∞	∞	0	∞	∞	∞	∞	∞	∞	∞	∞	∞	∞	∞	∞	∞	∞	∞	∞	∞	∞	∞	∞
14	∞	∞	∞	∞	∞	∞	∞	∞	∞	∞	∞	∞	∞	0	∞	∞	∞	∞	∞	∞	∞	∞	∞	∞	∞	∞	∞	∞	∞	∞	∞	∞	∞
15	∞	∞	∞	∞	∞	∞	∞	∞	∞	∞	∞	∞	∞	∞	0	∞	∞	∞	∞	∞	∞	∞	∞	∞	∞	∞	∞	∞	∞	∞	∞	∞	∞
16	∞	∞	∞	∞	∞	∞	∞	∞	∞	∞	∞	∞	∞	∞	∞	0	∞	∞	∞	∞	∞	∞	∞	∞	∞	∞	∞	∞	∞	∞	∞	∞	∞
17	∞	∞	∞	∞	∞	∞	∞	∞	∞	∞	∞	∞	∞	∞	∞	∞	0	∞	∞	∞	∞	∞	∞	∞	∞	∞	∞	∞	∞	∞	∞	∞	∞
18	∞	∞	∞	∞	∞	∞	∞	∞	∞	∞	∞	∞	∞	∞	∞	∞	∞	0	∞	∞	∞	∞	∞	∞	∞	∞	∞	∞	∞	∞	∞	∞	∞
19	∞	∞	∞	∞	∞	∞	∞	∞	∞	∞	∞	∞	∞	∞	∞	∞	∞	∞	0	∞	∞	∞	∞	∞	∞	∞	∞	∞	∞	∞	∞	∞	∞
20	1	∞	1	∞	∞	∞	∞	∞	∞	∞	∞	1	∞	∞	∞	∞	∞	∞	∞	0	∞	∞	∞	1	∞	∞	∞	∞	∞	1	∞	∞	∞
21	∞	∞	∞	∞	∞	∞	∞	∞	∞	∞	∞	∞	∞	∞	∞	∞	∞	∞	∞	∞	0	∞	∞	∞	∞	∞	∞	∞	∞	∞	∞	∞	∞
22	∞	∞	∞	∞	∞	∞	∞	∞	∞	∞	∞	∞	∞	∞	∞	∞	∞	∞	∞	∞	∞	0	∞	∞	∞	∞	∞	∞	∞	∞	∞	∞	∞
23	∞	∞	∞	∞	∞	∞	∞	∞	∞	∞	∞	∞	∞	∞	∞	∞	∞	∞	∞	∞	∞	∞	0	∞	∞	∞	∞	∞	∞	∞	∞	∞	∞
24	1	∞	1	∞	∞	∞	∞	∞	∞	∞	∞	1	∞	∞	∞	∞	∞	∞	∞	∞	∞	∞	∞	0	∞	∞	∞	∞	∞	1	∞	∞	∞
25	∞	∞	∞	∞	∞	∞	∞	∞	∞	∞	∞	∞	∞	∞	∞	∞	∞	∞	∞	∞	∞	∞	∞	∞	0	∞	∞	∞	∞	∞	∞	∞	∞
26	∞	∞	∞	∞	∞	∞	∞	∞	∞	∞	∞	∞	∞	∞	∞	∞	∞	∞	∞	∞	∞	∞	∞	∞	∞	0	∞	∞	∞	∞	∞	∞	∞
27	∞	∞	∞	∞	∞	∞	∞	∞	∞	∞	∞	∞	∞	∞	∞	∞	∞	∞	∞	∞	∞	∞	∞	∞	∞	∞	0	∞	∞	∞	∞	∞	∞
28	∞	∞	∞	∞	∞	∞	∞	∞	∞	∞	∞	∞	∞	∞	∞	∞	∞	∞	∞	∞	∞	∞	∞	∞	∞	∞	∞	0	∞	∞	∞	∞	∞
29	∞	∞	∞	∞	∞	∞	∞	∞	∞	∞	∞	∞	∞	∞	∞	∞	∞	∞	∞	∞	∞	∞	∞	∞	∞	∞	∞	∞	0	∞	∞	∞	∞
30	1	∞	1	∞	∞	∞	∞	∞	∞	∞	∞	1	∞	∞	∞	∞	∞	∞	∞	1	∞	∞	∞	1	∞	∞	∞	∞	∞	0	∞	∞	∞
31	∞	∞	∞	∞	∞	∞	∞	∞	∞	∞	∞	∞	∞	∞	∞	∞	∞	∞	∞	∞	∞	∞	∞	∞	∞	∞	∞	∞	∞	∞	0	∞	∞
32	∞	∞	∞	∞	∞	∞	∞	∞	∞	∞	∞	∞	∞	∞	∞	∞	∞	∞	∞	∞	∞	∞	∞	∞	∞	∞	∞	∞	∞	∞	∞	0	∞
33	∞	∞	∞	∞	∞	∞	∞	∞	∞	∞	∞	∞	∞	∞	∞	∞	∞	∞	∞	∞	∞	∞	∞	∞	∞	∞	∞	∞	∞	∞	∞	∞	0

of the designated battery are equal to 0.95 which is equal to a 0.9 round-trip efficiency. If the operation uses a battery with a higher level of efficiency, much more levels of the abovementioned benefits will be yielded. At last but not the least, by using mobile battery storage total energy losses of the network is reduced from 6288 kWh to 5333 kWh which is comparable with respect to the mobility costs.

Results of optimal scheduling of the mobile battery in the MBES case are shown in Table 4, Fig. 7, and Fig. 8. Hourly transport schedule of the mobile is illustrated in Table 4. The table conveys some important point as follows. The battery does not move the initial location, namely

Table 3
Total results of the simulations.

Case Title	BESS Status		Total Cost	Location	Total Cost Difference	
					$	%
NBESS	None		16,841	–	–	–
MBESS	**Mobile**		**16,158**	**Bus 1,30**	**683**	**4.06**
SBESS	Fixed	Min	16,569	Bus 1	273	1.62
		Average	16,351	System	490	2.91
		Median	16,285	Bus 33	556	3.30
		Max	16,232	Bus 30	609	3.60

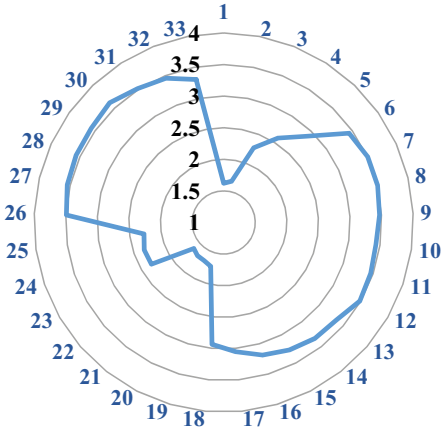

Fig. 6. . Operation cost reduction percent for SBESS case.

Table 4
Transport schedule of the mobile battery for MBESS case.

Time	Bus
1	1
2	1
3	1
4	1
5	1
6	Transport
7	30
8	30
9	30
10	30
11	30
12	30
13	30
14	30
15	30
16	30
17	30
18	30
19	30
20	30
21	30
22	30
23	Transport
24	1

bus 1, at the initial time periods of the operation. This is means that bus 1 is the best location for the battery in terms of starting charging periods. Afterwards, the battery stays at bus 3 for 5 h and is disconnected from the grid at hour 6 because it is being transferred. At hour 6 battery connects to bus 30 to perform discharging action. In the following and at hour 23 the battery leaves the network to return to its original position in bus 1.

Figure. 7 illustrates hourly charging and discharging schedule of the battery for MBESS case. In the figure, positive and negative values denote charging and discharging power, respectively. Also, Fig. 8 show stored energy in the mobile battery for any time period of operation. As the figures point out, the battery starts the time periods with charging action. This is because of two facts, shape of the load profile and zero initial energy of the battery. In other word, considering that the load profile starts with a valley in terms of electricity demand, the battery seizes the opportunity to draw energy by charging power. As the figure demonstrate, the battery will continue to charge for up to 4 h until it is fully charged.

Then moves to bus 30 to deliver charged energy at periods of peak loads, i.e., hours 16 to 21. As soon as the battery discharging periods begin, the energy stored in it is reduced to eventually reach the initial value of zero. By combining results of mobile battery location and power scheduling, one important point can be deduced as follows. The best locations for charging and discharging of the battery are buses 1 and 30, respectively. This can be interpreted as the battery in the charging state tends to be powered at the shortest distance from its source in the substation, i.e., bus 1. This minimizes the power losses of the lines while charging and thus reduces the total cost. On the other hand, the battery tends to be in the discharging state at the load center of the network so that the discharged energy is provided with the least distance from the load, which means that it is placed in bus 30.

Figs. 9-11 show active, reactive, and apparent power output of the substation for NBESS and MBESS cases. As Fig. 9 denotes, profile of the generated power is leveled because of optimal operation of the mobile battery. As the figure show, peak of the curve is clipped by delivering energy stored in the valley. The figure is accordance with the charging and discharging power of the battery presented in the previous figures. Fig. 10 depicts reactive power output of the substation for various time periods. As it can be concluded from the figure, reactive power injected by the battery greatly assisted to reduce the reactive power output of the substation. As a conclusion, apparent power output of the substation is shown in Figure. As it was expected, output power flow of the substation is considerably reduced because of reduction in the both active and reactive power. This, in turn, will defer expansion requirement of the substation.

A sensitivity analysis is performed to analysis functionality of the proposed model in managing various circumstances. At the first step, a different profile is used as hourly load factor. The profile which is shown in Fig. 12 is for an industrial area and with two peak periods. The purpose of using this load profile is to knew how the mobile battery will be scheduled considering two valleys and two peaks in the curve.

The result of hourly transport scheduling is shown in Table 5. As in was expected, as the bus loads diversity did not change, the origin and destination of the battery movement remained same as the previous load profile. However, hourly movements are changed according to the valley and peak periods of the new load profile. As in the table, the battery stays in bus 1 from the beginning of the operating period for 6 h. At these hours, the battery stores the energy needed to supply the first peak of the load curve. Then, at hour 7, it leaves the network to move to a new location. Due to the one-hour distance, it arrives at bus 30 at hour 8 to recharge the energy stored for supplying the first peak period. After that, the battery repeats this process for the next peak. For this purpose, it was moving during hour 13 to connect to the best place to recharge, namely bus 1. The battery lasts 4 h in bus 1 to charge required energy for the second stage. Then, at hour 18, it moves again to bus 30 and remains for 4 h to supply the second peak. Afterwards, the battery will make its third transport by moving back to its original location.

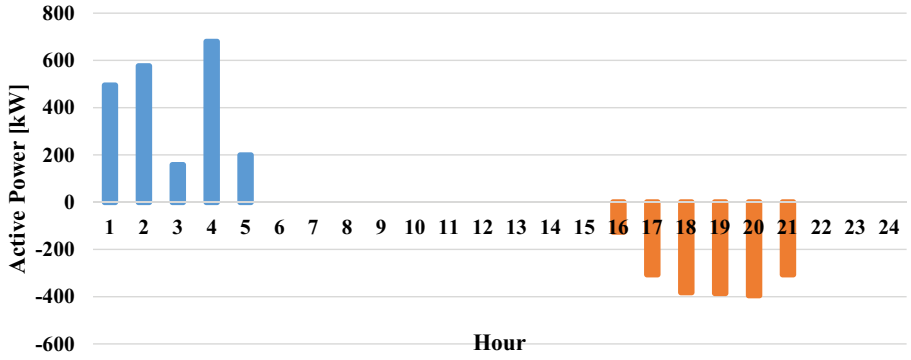

Fig. 7. Hourly charge/discharge schedule of the mobile battery for MBESS case.

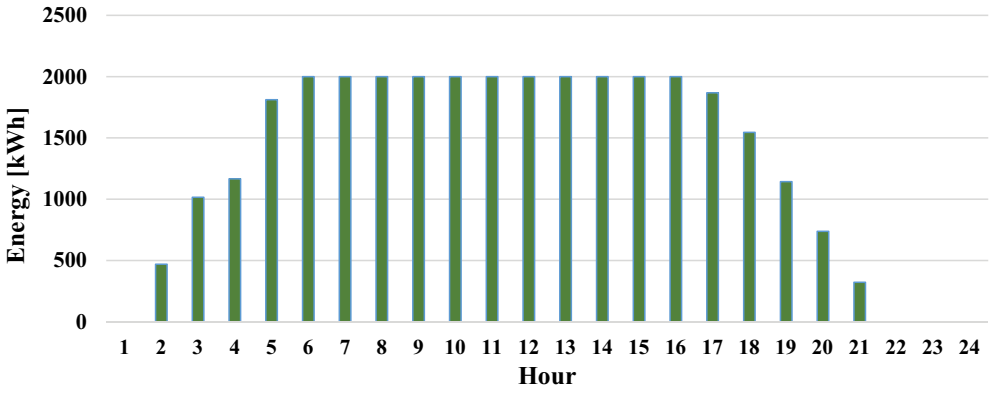

Figure 8. Stored energy in the mobile battery for MBESS case

Fig. 8. Stored energy in the mobile battery for MBESS case.

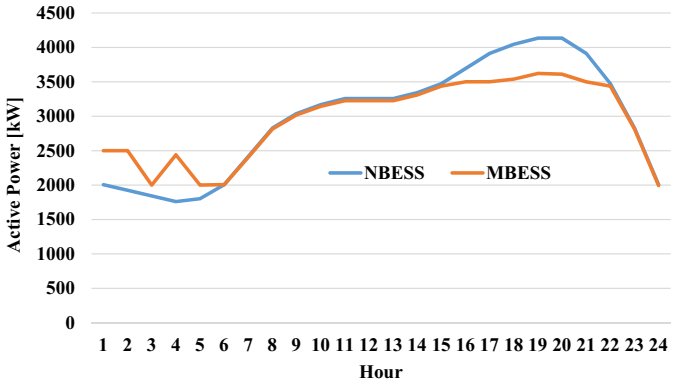

Fig. 9. Hourly active power generated by the substation for cases NBESS and MBESS.

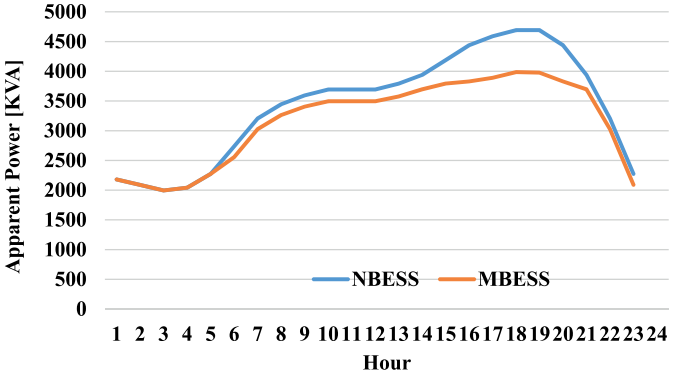

Fig. 11. Hourly apparent power generated by the substation for cases NBESS and MBESS.

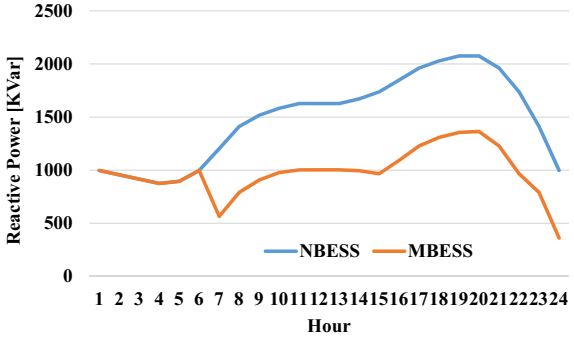

Fig. 10. Hourly reactive power generated by the substation for cases NBESS and MBESS.

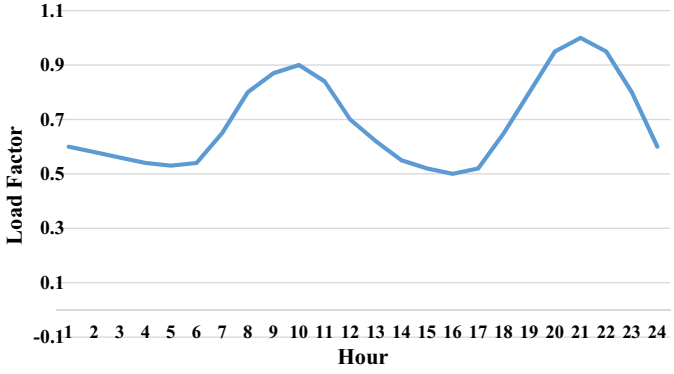

Fig. 12. Hourly load factors for industrial area.

The battery performs this last movement at hour 23 and finally be in its original location at the end of the operation period at hour 24. This movement scheduling for the mobile battery yields a 14,388$ operation cost. Total operation cost for this new load profile in the case without battery storage is 15,056$. This means a 676 $ net reduction in the operation cost corresponding to 4.493 percent. these values denote two points. The first one is to prove ability of the proposed model to find optimal scheduling of the mobile battery in various conditions. The second one is that the greater the amount and number of the load profile oscillations, the greater the advantages and benefits of using a mobile battery.

At last but not the least, effect of changing initial location of the mobile battery is analyzed. Table 6 shows the results for all possible locations of the battery at the beginning of the operation time window. As it can be observed, total operation cost is not changed considerably, but, number of movements is equal to 3 except for the base case. Also, operation cost for the case with battery initially located at bus 1 is the lowest one. Table 7 presents movement scheduling for all possible

Table 5
Transport schedule of the mobile battery for industrial load profile.

Time	Bus	
1	1	30
2	1	30
3	1	30
4	1	30
5	1	30
6	1	30
7	Transport	
8		30
9		30
10		30
11		30
12		30
13	Transport	
14	1	30
15	1	30
16	1	30
17	1	30
18	Transport	
19		30
20		30
21		30
22		30
23	Transport	
24	1	30

Table 6
Total cost results for MBESS case with various initial locations.

Initial Location	Total Cost	Difference		# of Transports
		$	%	
Bus 1	16,157.890	683.728	4.060	2
Bus 3	16,159.775	681.850	4.049	3
Bus 6	16,158.353	683.272	4.057	3
Bus 12	16,159.210	682.414	4.052	3
Bus 20	16,161.423	680.201	4.039	3
Bus 24	16,159.835	681.789	4.048	3
Bus 30	16,158.491	683.133	4.056	3

initial locations. As can be seen from the results, the battery has followed a similar transportation pattern, regardless of the initial location. In other word, in any case, the battery tends to charge at bus 1 and discharge at bus 30. Battery movement to bus 1 at the beginning of the time periods, as well as movement to bus 30 at hour 30 indicate this fact. Moreover, in all cases, the battery finally tries to place at its original location at hour 24 by performing a transportation at hour 23. The results also show the accuracy of the modeling performed and its efficiency in optimizing the real cases regardless of changing problem inputs.

4. Discussions

The model presented for the mobile battery operation can be easily integrated in the distribution planning tools. The computational burden of the problem is initially related to the size of the distribution network in which the problem is implemented. In addition, increasing number of segments in the piece-wise approximation used in the substation cost will increase problem accuracy at the expense of the run time. Furthermore, enhancing number of the side in the apparent polygon used for approximating line and battery apparent power flow limitation will also increase simulation run time.

As the simulation results show, the optimal use of the mobile battery by using the proposed model will reduce the cost of daily operation. The rate of daily cost reduction depends on several factors. The most important factor is the shape of the daily load profile. The shape of the load profile reflects the number of peak periods, the duration of each peak, as well as the power difference between peak and non-peak periods. In addition, the starting point of the battery movement in the daily operation schedule as well as its charging and discharging efficiency will affect the results. Although according to the results, the starting point does not have much effect on reducing the cost, but it reduces the number of mobile battery movements, which means reducing the cost of using the battery. It should be noted that the reduction in the cost of daily operation is due to both the arbitrage performed by the battery and the reduction in losses due to peak cutting.

Also, leveling the load profile by means of the battery will reduce losses, reduce voltage drop, and also reduce the loading of the lines and substations. Reducing the load on network equipment, in turn, means deferring the need for network expansions. Although these benefits are achievable with a stationary battery at some degrees, as simulation results show, the reduction in the daily cost of a mobile battery is greater than all possible stationary battery locations. In addition, mobile batteries can be used to achieve greater network expansion deferral levels as a result of much more peak shaving. In addition, as previous studies have shown, using a mobile battery in the event of an unexpected failure of the network equipment is one of the best ways to increase network resilience and reliability [16–20]. The simulation results show that mobile batteries have an advantage over stationary batteries not only in emergencies but also in normal operation for a small payment for two movements per day.

Finally, as mentioned earlier, the daily savings for the normal load profile will be 4.06% and for the industrial load profile with two peak periods will be 4.493%. Each of these figures means a net daily savings of 676 and 683 dollars, respectively. Assuming that the daily cost saving is proportional to the peak of the load profile of the day, and using the annual load profile of the IEEE RTS System, the total annual savings will be equal to 246,240 dollars. Assuming the battery costs $ 200 per kilowatt-hour (for typical power range), the total battery cost will be $ 400,000. The annual savings achieved compared to the cost of installing the battery are quite competitive.

5. Conclusions

Battery-powered energy storage devices possess transportability capability in power systems. This means that the battery can charge and discharge in different places. This will improve the battery functionality and increase their benefits. In this context, this paper presents a new method for optimally scheduling time-location management as well as charge-discharge for mobile batteries in the power distribution network. For this purpose, a new method for modeling the battery transport regardless of the transfer method was presented. The proposed model is a linear optimization model and can be applied to large-scale real networks. The results of model implementation at the base case show a reduction of more than 4% of the daily operating cost for a typical load pattern. This value is increased by about 0.5% for the industrial load pattern with two peak periods. The battery also coordinates itself well with the number of peak periods. The sensitivity analysis results also demonstrate that the battery moves to the vicinity of the power source at the charging state as well as being in the load center at the discharge state. As a trend for the future works, mobile battery can be compared with the other mobile resources in the networks, for example generators. In addition, mobile battery operation optimization can be compared with the coordinated management of the electric vehicles' batteries.

Table 7
Transport schedule of the mobile battery for MBESS case with various initial locations.

Initial Location	Bus 1			Bus 3			Bus 6			Bus 12			Bus 20			Bus 24			Bus 30	
Movement Pattern	Bus			Bus			Bus			Bus			Bus			Bus			Bus	
1	1				3			6			12			20			24			30
2	1			Transport			Transport			Transport			Transport			Transport			Transport	
3	1			1			1			1			1			1			1	
4	1			1			1			1			1			1			1	
5	1			1			1			1			1			1			1	
6	Transport			Transport			Transport			Transport			Transport			Transport			Transport	
7		30				30			30			30			30			30		30
8		30				30			30			30			30			30		30
9		30				30			30			30			30			30		30
10		30				30			30			30			30			30		30
11		30				30			30			30			30			30		30
12		30				30			30			30			30			30		30
13		30				30			30			30			30			30		30
14		30				30			30			30			30			30		30
15		30				30			30			30			30			30		30
16		30				30			30			30			30			30		30
17		30				30			30			30			30			30		30
18		30				30			30			30			30			30		30
19		30				30			30			30			30			30		30
20		30				30			30			30			30			30		30
21		30				30			30			30			30			30		30
22		30				30			30			30			30			30		30
23	Transport			Transport			Transport			Transport			Transport			Transport				30
24	1				3			6	30		12			20			21			30

Appendix

A.1. Battery life-time modeling

One of the issues related to the operation of batteries is their life time. Batteries are among the energy storage devices whose life time depends on various conditions. Among the most important of them is the depth of discharge and also the number of repetitions of the charge and discharge cycle. Various models have been used to consider battery life. One of the most straightforward of these models is given below [36]. In his regard, battery life time degradation will be modeled as a daily degradation cost in the objective function. The operation model of the mobile battery will be as follows, taking into account the life time degradation cost.

$$TC = \sum_{g,t} C^{NG}_{(g,t)} + \sum_{i,t} C^{LS}_{(i,t)} + \sum_{i} \sum_{t} \left(\left| \frac{h}{100} \right| C^{P} (P^{BC}_{(i,t)} + P^{BD}_{(i,t)}) \right) \tag{45}$$

The degradation cost is calculated based on the model introduced in [34]. The parameter C^P is power rating cost of the battery and parameter h is technology-specific degradation slope.

A.2. CPLEX Solver

Although CPLEX optimizer uses other types of mathematical optimization methods and interfaces, it was named because of using simplex method in the C language. This powerful tool can solve very large scale linear programming problems using primal or dual simplex method or interior point method. Integer programming problems using branch and bound method, convex in addition to the non-convex quadratic programming problems, and convex quadratically constrained problems (second-order cone programming, or SOCP). Although the CPLEX offers interface to C++, C#, and Java languages, it can be connected to Microsoft Excel or MATLAB and is also within independent optimization modeling systems such as GAMS, AMPL, AIMMS, OptimJ, or TOMLAB. GAMS/ CPLEX provides the users high level modeling facilities of GAMS combined with the capabilities of CPLEX optimizers, namely powerful solve procedures for vary large and difficult problems quickly and with minimal user involvement.

References

[1] S. Koohi-Fayegh, M.A. Rosen, "A review of energy storage types, applications and recent developments", J. Energy Storage 27 (2020) 101047.

[2] S.U. Agamah, L. Ekonomou, "Peak demand shaving and load-levelling using a combination of bin packing and subset sum algorithms for electrical energy storage system schedulin. IET Sci. Meas. Technol. 10 (5) (2016) 477–484.

[3] S.U. Agamah, L. Ekonomou, "Energy storage system scheduling for peak demand reduction using evolutionary combinatorial optimisation.", Sustain. Energy Technol. Assess. 23 (2017) 73–82.

[4] M. Nazari-Heris, F. Kalavani, Evaluation of peak shifting and energy saving potential of ice storage based air conditioning systems in Iran, J. Oper. Autom. Power Eng. 5.2 (2017) 163–170.

[5] A. Nieto, V. Vita, I Theodoros, Maris, Power quality improvement in power grids with the integration of energy storage systems, Int. J. Eng. Res. Technol. 5.7 (2016) 438–443.

[6] R. Hemmati, H. Saboori, "Emergence of hybrid energy storage systems in renewable energy and transport applications–A review, Renew. Sustain. Energy Rev. 65 (2016) 11–23.

[7] M. Nazari-Heris, et al., Optimal stochastic scheduling of virtual power plant considering NaS battery storage and combined heat and power units, J. Energy Manag. Technol. 2.3 (2018) 1–7.
[8] J. Figgener, P. Stenzel, K.P. Kairies, J. Linßen, D. Haberschusz, O. Wessels, G. Angenendt, M. Robinius, D. Stolten, D.U. Sauer, The development of stationary battery storage systems in Germany–A market review, J. Energy Storage 29 (2020) 101153.
[9] Holger C. Hesse, Michael Schimpe, Daniel Kucevic, Andreas Jossen, "Lithium-ion battery storage for the grid—A review of stationary battery storage system design tailored for applications in modern power grids, Energies 10 12 (2017) 2107.
[10] The Business Case for Mobile Batteries in New York. Available online at:www.greentechmedia.com/.
[11] Y. Sun, Z. Li, M. Shahidehpour, B. Ai, "Battery-based energy storage transportation for enhancing power system economics and security, IEEE Trans. Smart Grid 6 5 (2015) 2395–2402.
[12] Y. Sun, Z. Li, W. Tian, M. Shahidehpour, A Lagrangian decomposition approach to energy storage transportation scheduling in power systems, IEEE Trans. Power Syst. 31 6 (2016) 4348–4356.
[13] Y. Sun, J. Zhong, Z. Li, W. Tian, M. Shahidehpour, Stochastic scheduling of battery-based energy storage transportation system with the penetration of wind power, IEEE Trans. Sustain. Energy 8 1 (2016) 135–144.
[14] Y. Zheng, Z. Dong, S. Huang, K. Meng, F. Luo, J. Huang, D. Hill, "Optimal integration of mobile battery energy storage in distribution system with renewables, J. Mod. Power Syst. Clean Energy 3 4 (2015) 589–596.
[15] Y. Zheng, K. Meng, F. Luo, J. Qiu, J. Zhao, Optimal integration of MBESSs/SBESSs in distribution systems with renewables, IET Renew. Power Gener. 12 10 (2018) 1172–1179.
[16] Y. Wang, C. Chen, J. Wang, R. Baldick, Research on resilience of power systems under natural disasters—A review, IEEE Trans. Power Syst. 31 2 (2015) 1604–1613.
[17] M. Panteli, D.N. Trakas, P. Mancarella, N.D. Hatziargyriou, "Power systems resilience assessment: hardening and smart operational enhancement strategies, Proc. IEEE 105 7 (2017) 1202–1213.
[18] J. Kim, Y. Dvorkin, Enhancing distribution system resilience with mobile energy storage and microgrids, IEEE Trans. Smart Grid (2018).
[19] S. Yao, P. Wang, T. Zhao, Transportable energy storage for more resilient distribution systems with multiple microgrids, IEEE Trans. Smart Grid (2018).
[20] S. Lei, C. Chen, H. Zhou, Y. Hou, Routing and scheduling of mobile power sources for distribution system resilience enhancement, IEEE Trans. Smart Grid 10 5 (2018) 5650–5662.
[21] M. Khan, A. Tanvir, et al., Dynamic modeling and feasibility analysis of a solid-state transformer-based power distribution system, IEEE Trans. Ind. Appl. 54 1 (2017) 551–562.
[22] H. Mehrjerdi, R. Hemmati, Modeling and optimal scheduling of battery energy storage systems in electric power distribution networks, J. Clean. Prod. (2019).
[23] H. Mehrjerdi, Simultaneous load leveling and voltage profile improvement in distribution networks by optimal battery storage planning, Energy (2019).
[24] M. Nazari-Heris, et al., Optimal stochastic scheduling of virtual power plant considering NaS battery storage and combined heat and power units, J. Energy Manag. Technol. 2 3 (2018) 1–7.
[25] H. Saboori, et al., Energy storage planning in electric power distribution networks–A state-of-the-art review, Renew. Sustain. Energy Rev. 79 (2017) 1108–1121.
[26] A.J. Wood, B.F. Wollenberg, G.B. Sheblé, Power Generation, Operation, and Control (2013).
[27] Sortomme, E., and M.A. El-Sharkawi. "Optimal power flow for a system of microgrids with controllable loads and battery storage." Proceedings of the IEEE/PES Power Systems Conference and Exposition. IEEE, 2009.
[28] M. Khan, A. Tanvir, et al., Coordinated control of energy storage in networked microgrids under unpredicted load demands, Proceedings of the American Control Conference (ACC), IEEE, 2019.
[29] H. Saboori, R. Hemmati, S.M.S. Ghiasi, S. Dehghan, "Energy storage planning in electric power distribution networks–A state-of-the-art review, Renew. Sustain. Energy Rev. 79 (2017) 1108–1121.
[30] Z. Yang, H. Zhong, A. Bose, T. Zheng, Q. Xia, C. Kang, A linearized OPF model with reactive power and voltage magnitude: a pathway to improve the MW-only DC OPF, IEEE Trans. Power Syst. 33 (2018) 1734–1745.
[31] Z. Yang, H. Zhong, Q. Xia, C. Kang, Solving OPF using linear approximations: fundamental analysis and numerical demonstration, IET Gener. Transm. Distrib. 11 17 (2017) 4115–4125.
[32] M.E. Baran, F.F. Wu., Network reconfiguration in distribution systems for loss reduction and load balancing, IEEE Trans. Power Deliv. 4 2 (1989) 1401–1407.
[33] Y. Zhang, S. Ren, Z.Y. Dong, Y. Xu, K. Meng, Y. Zheng, "Optimal placement of battery energy storage in distribution networks considering conservation voltage reduction and stochastic load composition, IET Gener. Transm. Distrib. 11 15 (2017) 3862–3870.
[34] Cplex, I.L.O.G. "11.0 User's manual." ILOG SA, Gentilly, France (2007): 32.
[35] A. Brook, D. Kendrick, A. Meeraus, "GAMS, a user's guide, ACM Signum Newsletter 23 3-4 (1988) 10–11.
[36] M.A. Ortega-Vazquez, Optimal scheduling of electric vehicle charging and vehicle-to-grid services at household level including battery degradation and price uncertainty, IET Gener. Transm. Distrib. 8 (6) (2014) 1007–1016.